Remote Sensing of Environment 115 (2011) 269–280

Contents lists available at ScienceDirect

Remote Sensing of Environment

journal homepage: www.elsevier.com/locate/rse

Spatial scaling of stable night lights

Christopher Small [a,*], Christopher D. Elvidge [b], Deborah Balk [c], Mark Montgomery [d]

[a] Lamont Doherty Earth Observatory, Columbia University, Palisades, NY 10964, USA
[b] Earth Observation Group, NOAA National Geophysical Data Center, Boulder, CO 80303, USA
[c] Baruch College, City University of New York & CUNY Inst. for Demographic Research, NY, NY 10010, USA
[d] Department of Economics, Stony Brook University, Stony Brook, NY 11794, USA

ARTICLE INFO

Article history:
Received 5 May 2010
Received in revised form 10 August 2010
Accepted 28 August 2010

Keywords:
Urban
Land cover
Night light
Landsat
Zipf
Power law
Scaling

ABSTRACT

City size distributions, defined on the basis of population, are often described by power laws. Zipf's Law states that the exponent of the power law for rank-size distributions of cities is near −1. Verification of power law scaling for city size distributions at continental and global scales is complicated by small sample sizes, inappropriate estimation techniques, inconsistent definitions of urban extent and variations in the accuracy and spatial resolution of census administrative units. We attempt to circumvent some of these complications by using a continuous spatial proxy for anthropogenic development and treat it as a spatial complement to population distribution. We quantify the linearity and exponent of the rank-size distribution of spatially contiguous patches of stable night light over a range of brightnesses corresponding to different intensities of development. Temporally stable night lights, as measured by the Defense Meteorological Satellite Program-Operational Line Scanner (DMSP-OLS), provide a unique proxy for anthropogenic development. Brightness and spatial extent of emitted light are correlated to population density (Sutton et al., 2001), built area density (Elvidge et al., 2007c) and economic activity (Doll et al., 2006; Henderson et al., 2009) at global scales and within specific countries. Using a variable brightness threshold to derive spatial extent of developed land area eliminates the complication of administrative definitions of urban extent and makes it possible to test Zipf's Law in the spatial dimension for a wide range of anthropogenic development. Higher brightness thresholds generally correspond to more intense development while lower thresholds extend the lighted area to include smaller settlements and less intensively developed peri-urban and agricultural areas. Using both Ordinary Least Squares (OLS) and Maximum Likelihood Estimation (MLE) to estimate power law linearity and exponent of the resulting rank-size distributions across a range of upper tail cutoffs, we consistently find statistically significant exponents in the range −0.95 to −1.11 with an abrupt transition to very large, extensively connected, spatial networks of development near the low light detection limit of the sensor. This range of exponents and transition are observed at both continental and global scales. The results suggest that Zipf's Law also holds for spatial extent of anthropogenic development across a range of intensities at both continental and global scales. The implication is that the dynamics of urban growth and development may be represented as spatial phase transitions when the spatial extent and intensity of development are treated as continuous variables rather than discrete entities.

© 2010 Published by Elsevier Inc.

1. Introduction

Understanding of urban growth processes is challenged by the large number of variables known to influence these processes. Despite the need for large sample sizes, most comparative studies of urban growth use only a subset of the world's cities and many studies focus on a single city or small number of cities for specific time intervals. Almost all of these studies rely on administratively defined clusters of population. Understanding of the processes is further complicated by the lack of any widely accepted and consistent definition of what constitutes a city or urban area (United Nations, 2008). In spite of these challenges, some consistency has been observed in the size distribution of populations of cities. (Auerbach, 1913) observed that the size distribution for cities can often be described as a power law in which the number of cities with population greater than N is inversely proportional to N. Zipf (1949) noted that the exponent of the power law is also close to −1 for the frequency of usage of words and postulated a universal principal of least effort on the basis of these observations. The special case of a power law distribution with an exponent of −1 is generally referred to as Zipf's Law and has been tested repeatedly by economists, geographers, urbanists and physicists. Gabaix (1999) states "Zipf's law for cities is one of the most conspicuous empirical facts in economics—or in the social sciences generally. The importance of this law is that, given very strong

* Corresponding author. Tel.: +347 535 4274.
E-mail address: small@LDEO.columbia.edu (C. Small).

0034-4257/$ – see front matter © 2010 Published by Elsevier Inc.
doi:10.1016/j.rse.2010.08.021

empirical support, it constitutes a minimum criterion of admissibility for any model of local growth or any model of cities".

Despite considerable research on Zipf's Law for cities, and numerous proposed explanations, there appears to be no consensus on the cause or even the generality of the law. The power law is used to describe only the upper tail of the distribution with varying criteria used for selecting a lower cutoff. While there have been challenges to the validity of Zipf's Law (e.g. Gan et al., 2006; Nitsch, 2005), numerous examples have been found for city size distributions within specific countries over the past 100 years in which the law appears to hold remarkably well (see Gabaix et al., 2004 and Pumain, 2004) for summaries). However, the exponent appears to vary from country to country (e.g. Pumain and Moriconi-Ebrard, 1997), and even within the same country over time (Guérin-Pace, 1995; Overman and Ioannides, 2001). To complicate matters further, the value of the exponent depends on the method of estimation (Rosen and Resnick, 1980; Soo, 2005). An underlying cause of many of these discrepancies is the difficulty of mapping human population. The purpose of this analysis is to explore a spatial complement to population distribution and to quantify some characteristics of the size distribution of human settlements at continental to global scales on the basis of a continuum of intensity of development (as defined below). This analysis tests the spatial manifestation of Zipf's law using an alternative measure of urbanness—nighttime lights. We use the concept of a continuum of anthropogenic development to avoid arbitrary definitions of urban land cover and to represent varying degrees of spatial connectivity among cities and other types of anthropogenic land cover.

2. Urban population and spatial extent

Much of the debate about the existence and generality of Zipf's Law seems to arise from two confounding factors related to how cities are defined and measured. The lack of a consistent definition of a city makes it difficult to compare size distributions between different countries (e.g. Pumain, 2004) because census enumerations depend on the administrative boundaries defined for each city and different countries have different, and often multiple, criteria for urban administrative boundaries.[1] The same factor confounds global analyses because inconsistency in definition precludes simple aggregation of tabular census data from different countries. A second confounding factor arises in the measurement of city size in terms of population.[2] Although administrative units are defined on the basis of spatial boundaries, the enumerations are implicitly aspatial because they discretize what are often spatially contiguous populated areas. Furthermore, cities can be defined according to different criteria—such as the population size, population density of functional criteria such as capitol cities or whether a given fraction of the labor force in engaged in non-agricultural activities. Remarkably, across time and place, the number of inhabitants has been a much more difficult criterion to measure consistently than one might imagine. As a result, there is no existing globally spatially-delineated population time-series for urban areas (Balk, 2009).

In fact, the idea of defining a city as a discrete entity with fixed boundaries may be fundamentally flawed because so many of the factors that characterize the form and function of human settlement patterns and dynamics are temporally variable over spatial gradients at some range of scales—such as, population density, housing density, road density, energy consumption, economic activity and output, emission and pollutant output. The fractal nature of urban development (Batty and Longley, 1994) combined with ubiquitous gradients in spatial density or intensity of development makes it difficult, and perhaps misleading, to define cities as discrete entities with fixed boundaries. Rather than considering the city as a single discrete entity defined in terms of inhabitants within an administrative boundary, we consider multiple spatial extents of anthropogenic land surface modification defined on the basis of varying degrees or intensities of development.

Human settlement patterns and, more generally, land surface modification can be represented as continuous spatial variation in intensity of development or degree of modification. A continuous depiction accommodates gradients while still allowing for sharp discontinuities observed in many cases (e.g. coastlines). A spatially and temporally continuous measure of the "degree of urbanness" provides a more general representation of many spatial and temporal processes while avoiding potential errors of omission and commission that inevitably result from discretization. Continuous variates also allow for the construction of different application-specific metrics from measurable quantities (e.g. those mentioned above) without the need to define a single discrete boundary separating urban from non-urban.

Numerous studies have attempted to elude the problem of urban definition by aggregating spatially adjacent population counts (see Pumain, 2006) but relatively few studies have attempted to investigate Zipf's Law in terms of area or spatial extent of anthropogenic land use—either within individual countries or aggregated to global scales. A recent study by (Rozenfeld et al., 2008) used spatially aggregated census data to demonstrate that urban agglomerations in the U.S.A. and Great Britain can be accurately described by Zipf's Law in terms of both population and area. Their results suggest that the exponent is sensitive to the scale length of the aggregation. At finer spatial scales (Fragkias and Seto, 2009) used satellite-derived urban extents of several cities in southern China to quantify temporal evolution of rank-size distributions revealing oscillations related to birth and spatial coalescence of settlements through time. Together these studies illustrate a spatial dimension to Zipf's Law that is often implied in studies using population data but rarely addressed explicitly.

As an alternative to discrete, population-based definitions of urban extent we consider a continuous, spatially explicit metric for anthropogenic land surface modification—analogous to population density—and investigate the effects of discretizing the metric at different levels or degrees of modification. Discretizing by imposing a threshold on the intensity of development results in a spatially segmented binary image with contiguous patches of developed area against an undeveloped (or less developed) background. Different thresholds result in different spatial distributions of developed area with different degrees of connectivity. Treating the size distribution of contiguous segments resulting from each threshold as a distinct depiction of anthropogenically modified or developed land area, we quantify the degree to which the spatial extent and distribution of human habitation and land surface modification can be described by a power law and how the parameters of the power law depend on the level of discretization.

3. Anthropogenic land use and night light

It is important to emphasize the difference between population counts and developed land area. Although night light brightness and population density are correlated at high levels, the relationship is less direct at the lowest brightness levels. In part, this is a result of overglow (discussed below) but also because of the variety of different sources that contribute to the lowest levels of detectable light. In this study we use satellite-derived observations of stable anthropogenic light as an indication of varying degrees of development

[1] National statistical offices not only vary in the census and administrative boundary that they collect, but also what they release, with the latter often being far more coarse than the former.

[2] In addition to variations in census accuracy and detail from country to country, most census enumerations quantify where people sleep rather than where they work and interact during the day.

and human habitation. What we refer to here as intensity of development corresponds to both the fractional area of the pixel occupied by human constructed surfaces and the brightness at which it is lit. The brightest pixels observed generally correspond to fully developed mixed use urban areas with near total outdoor illumination. Less brightly lit pixels may correspond to lower built area density with dimmer outdoor lighting throughout or to a small number of discrete lighted areas with somewhat brighter lighting. Pixels at the lowest brightness levels may correspond to a still wider variety of sources ranging from vehicle headlights, leakage from dwellings and still lower numbers of lighted outdoor areas within the instantaneous field of view of the pixel. The lowest detectable light levels may also result from the phenomenon of "overglow" discussed below. The comparisons in the next section illustrate the distinction between brightly lit urban centers and more dimly lit peri-urban and rural areas. The implications of this diversity of sources are considered in the discussion.

The Defense Meteorological Satellite Program Operational Line Scanner (DMSP-OLS) has been imaging night lights since the early 1970s (Croft, 1973). The more recent digital data have been used to produce annual global composites of temporally stable nighttime lights from 1992 to 2008 (Elvidge et al., 2001). The DMSP-OLS visible band was designed to detect moonlit clouds at night. It uses a photomultiplier tube to intensify the visible band signal by a million fold. This enables the detection of both moonlit clouds and lighting present at the Earth's surface. NGDC has developed procedures to make cloud-free annual composites of the nighttime visible band DMSP-OLS data (Elvidge et al., 2001). The result is a set of composite images in which each 30 arc second (~1 km at the equator) pixel gives the annual average brightness level in units of 6 bit digital numbers (DN) spanning the range 0 to 63. Additional procedures are used to remove ephemeral lights (mostly fires) and background noise to produce gridded stable lights products. The data are available for download from: http://www.ngdc.noaa.gov/dmsp/downloadV4composites.html (access 2 August, 2010).

Night lights are known to overestimate the spatial extent of development at the periphery of settlements (Elvidge et al., 1997). Imhoff et al. (1997) proposed the use of a low light threshold of 89%

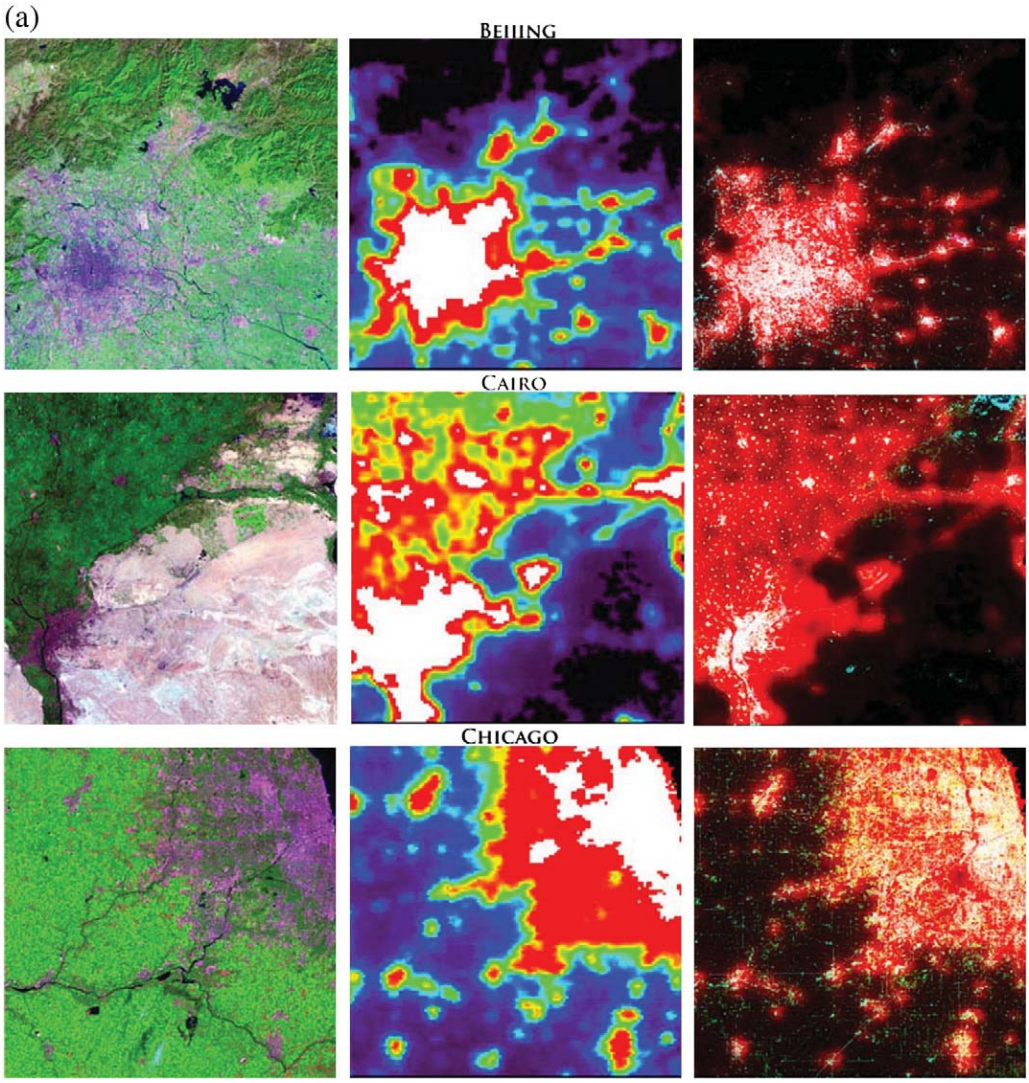

Fig. 1. a,b Urban–rural land cover gradients in reflected and emitted lights. Landsat 5 false color composites (left column) circa 2008 show developed, agricultural and undeveloped land cover. Homogeneous green areas are agriculture while the dark pink, purple and gray areas are generally associated with mixtures of SWIR-bright building materials and deep shadow characteristic of more intensive development. Stable night light brightness (center column) for 2008 ranges from dim low DN values (purple to cyan) to brighter (green to red) and saturated (white). Unlighted areas (black) are undeveloped. Day–night composites (right column) combine Landsat and night lights to illustrate consistencies in land cover and night light brightness. Superimposed night light brightness (red) on upper (green) and lower (blue) bounding estimates of built up extent show high density built environments (white) associated with bright night lights while agriculture and low density rural land cover are associated with lower light levels (DN<~20).

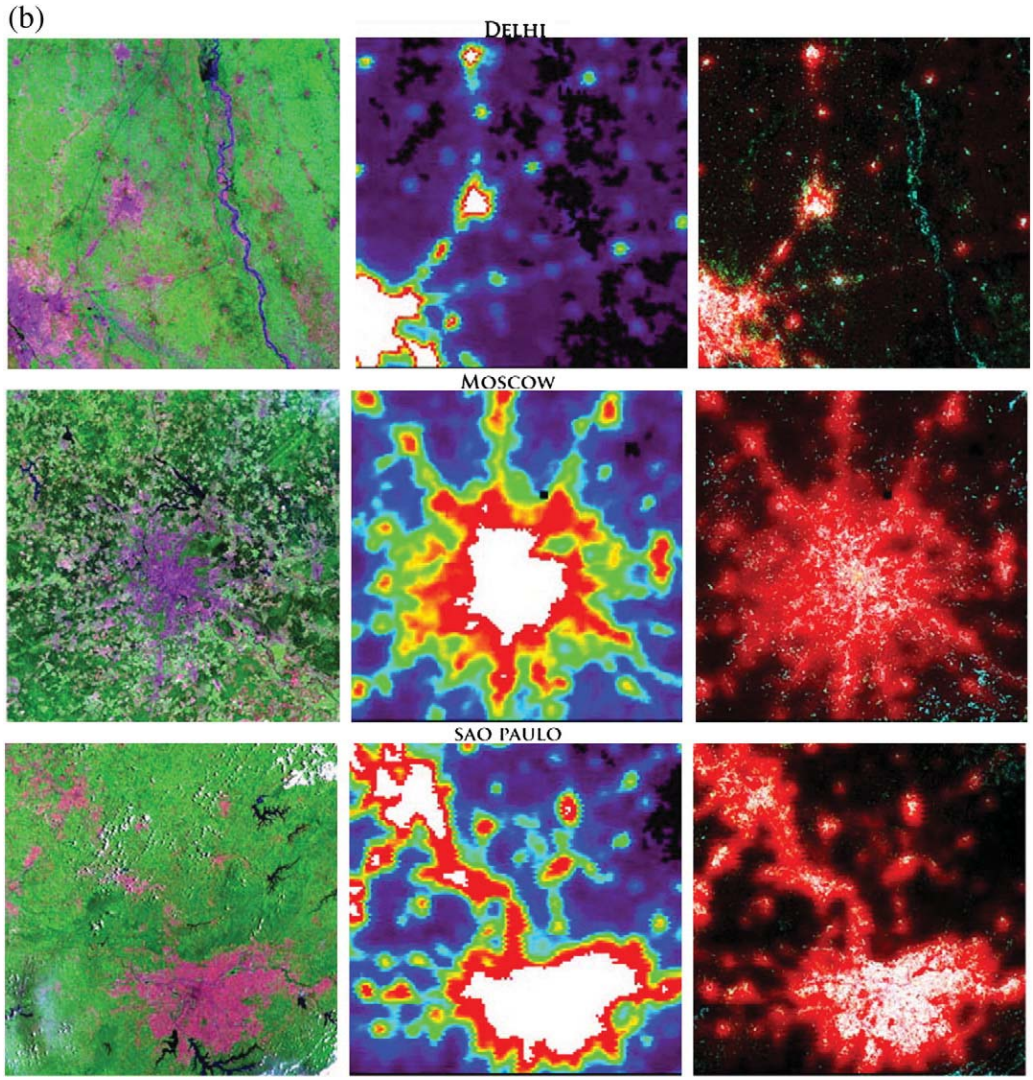

Fig. 1 (*continued*).

(applied to frequency of detection rather than brightness) to reduce the effects of overglow and shrink the spatial extent of the lighted area to better match the administrative extent of three U.S. cities. In a comparison of Landsat and night lights for 16 cities worldwide, Small et al. (2005) showed that differences in urban form and intensity of lighting (discussed below) preclude the use of a single threshold for all cities and that thresholding at the high levels proposed by Imhoff et al. (1997) results in the complete attenuation of large numbers of smaller settlements. Comparisons of stable light with 30 m resolution Landsat imagery on a wide variety of population density gradients indicates that average brightness increases with increasing spatial density of Shortwave Infrared reflectance and shadow associated with constructed surfaces (Small et al., 2005) as well as actual maps of impervious surfaces (Elvidge et al., 2007a,b,c). Example comparisons in Fig. 1 illustrate the spatial correspondence of dim lights (DN<~12) with agricultural and low population density land use while average brightness increases with both settlement size and intensity of development along urban–rural gradients. The spatial extent of the overglow is usually greater than the extent of high density impervious surface but it does not generally extend into areas that are completely undeveloped—except along coastlines. Comparisons with higher resolution images (see: www.LDEO.columbia.edu/~small/NightDay) indicate that the dimly lit areas with DN<~12 almost always contain some indication of anthropogenic land cover (e.g. agriculture), even when not coincident with high spatial densities of impervious surface typically associated with urban development. We discuss the implications of overglow and other artifacts below.

Brightness of stable lights is also correlated with population density at global scales (Sutton et al., 1997, 2001) although comparisons with census data are subject to the same complications discussed above. Despite these caveats, night lights offer a consistent global measure of the spatial extent of human habitation, development and intensity of economic activity. While brightness and spatial extent of night lights depend on a variety of socioeconomic and cultural factors (Elvidge et al., 2009), at global scales night lights provide a unique indicator of the distribution of human habitation and intensity of anthropogenic land use. As such, night lights provide a means to quantify the size, number and spatial extent of human settlements worldwide thereby allowing Zipf's Law to be tested using a proxy that is both independent of and complementary to the population counts used in previous studies. To our knowledge, only the analysis of Decker et al. (2007) has used night lights to test Zipf's Law—but found power law exponents between −0.73 and −0.89 and better fit by lognormal distributions. In contrast to Decker et al. (2007), we use a new, reprocessed and intercalibrated version of the night lights and we quantify the size distribution of contiguously lighted areas for different low light thresholds corresponding to different degrees of economic activity or development along urban–rural gradients.

4. Power law scaling of continuous fields

In this analysis, we avoid the problem of defining a discrete urban area by treating the intensity and corresponding spatial extent of development as a variable given by the average brightness of stable night light. This allows us to test Zipf's Law for developed land area at both global and regional scales for a range of different levels of urban development by varying the low light threshold designating the spatial extent of contiguous development. A benefit of this approach lies in its ability to quantify changes in spatial connectivity associated with different levels of development. As the low light threshold is increased from dim to bright the spatial extent of each segment (spatially contiguous patch) of developed land area shrinks and the overall size distribution changes as large agglomerations bound together by dimmer lights fragment and the smallest, dimmest lights are attenuated as they are exceeded by the threshold. The degree to which the resulting segment size distribution conforms to a power law can be used to quantify these changes in the distribution of spatially contiguous patches of developed land area for different thresholds defining different degrees of development. The change in the exponent, misfit and optimal lower tail cutoff with increasing low light threshold quantify the degree to which each corresponding segment size distribution conforms to a power law in general and Zipf's Law specifically. This provides a general approach to quantifying the aggregate spatial structure of a continuous field in terms of spatial connectivity, number and size distribution of local maxima.

Rather than treat the power law exponent as a single canonical metric, we acknowledge its potential sensitivity to how the quantity (e.g. city size) is defined and treat the defining criterion (e.g. low light threshold) as a variable to characterize the sensitivity of the size distribution. We calculate the size distribution of spatially contiguous lighted areas above each brightness threshold by segmenting the global composite mean brightness image for 2008 on the basis of spatial connectivity of each 1 km equal area pixel to its four cardinal near neighbors. The result is a set of spatially contiguous patches of land area exceeding the threshold brightness. We then calculate the total area of each distinct contiguous lighted segment and tabulate the size distribution for all segments (contiguous patches) for DN thresholds of 3, 5, 6, 7, 8, 9, 10, 11, 12, 14, 16, 20, 40 and 60. Because the resulting segments or contiguous patches of lighted area are increasingly diverse aggregations of brightly lighted urban cores, dimly lit rural areas and intermediate brightness suburban gradients we refer to the discrete patches as either segments or agglomerations, depending on the context.

The dependence of global agglomeration size distribution on low light brightness threshold is illustrated in Fig. 2. The inset area-brightness histogram (upper right) shows that the majority of lighted area on Earth is dimly lit (DN<20) so small changes in the low light threshold can result in large changes in lighted area. As the threshold is increased the combined effects of fragmentation and attenuation are apparent in the rank-size distributions (center). As shown, increasing the DN threshold from 3 (blue) to 8 (green) to 12 (red) diminishes the slope of the distribution (exponent of the power law) and reduces the size difference between the largest and smallest agglomerations. Higher thresholds from 20 to 40 to 60 (i.e., compare the magenta and black lines, respectively) increase the curvature of

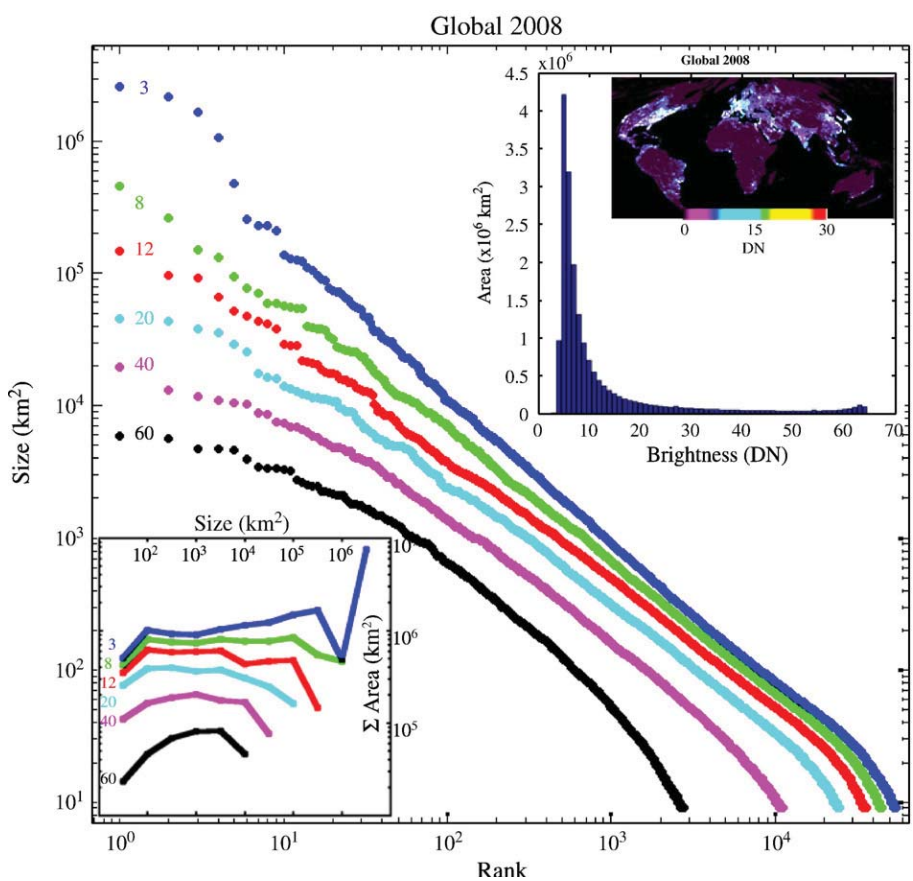

Fig. 2. Effect of low light thresholding on rank-size distribution of spatially contiguous lighted areas. Upper inset histogram shows most stable lights are relatively dim (low DN). Increasing the low light threshold from 3 to 60 attenuates smaller lights while fragmenting larger agglomerations connected by dimmer regions. This results in increasing curvature of the rank–size distributions. Lower inset histograms sum the total area of all lights within each size bin illustrating the net effect of attenuation and fragmentation for increasing brightness threshold. Note the nearly uniform distribution of total area over 3 orders of magnitude in size for the DN = 8 threshold while the lower DN threshold results in increasing dominance of the largest agglomerations.

the distribution—both diminishing the slope of the upper tail while drastically increasing the slope of the lower tail. Visually, the distributions resulting from low light thresholds are considerably more linear (down to sizes of a few tens of square kilometers) than those associated with the high thresholds that eliminate large areas of less developed land. The consequences of increasing the low light threshold are also apparent in the total integrated areas for different size classes of agglomeration. Rather than count the number of spatially contiguous agglomerations for different size range, the inset area-size histograms count the total area of each size range. The effect of increasing low light threshold in this case is to reduce the total area of both the largest and smallest agglomerations by fragmentation and attenuation respectively. Note however that the total area is nearly uniform across 3 orders of magnitude in size for a threshold of DN = 8 while the total area actually increases with size for the lowest threshold of DN = 3. The threshold of DN = 8 corresponds to a transition where the size distribution goes from being dominated by medium size (10^2 to 10^4 km^2) areas at higher thresholds to being strongly dominated by the largest size areas for lower thresholds. This has profound implications as discussed below.

Several previous analyses of city population size distributions (e.g. Rosen and Resnick, 1980; Soo, 2005) and other purported power laws (e.g. Newman, 2005; Clauset et al., 2009) indicate that the estimate of the exponent can be sensitive to biases inherent in the method of estimation. In this study we use both Ordinary Least Squares (OLS) on Log_{10} transformed rank and size (km^2) as well as the Maximum Likelihood Estimate (MLE) for a power law distribution of segment sizes. Although the OLS approach is, by far, the more commonly used method for estimation of Zipf exponents, it suffers from a number of shortcomings as a means of quantifying and testing the power law hypothesis (Clauset et al., 2009; Newman, 2005; Sornette, 2003). We use OLS merely for intuitive illustration and comparison with more statistically sound estimates of the power law exponent, optimal size cutoff, uncertainty and goodness of fit derived using the MLE and semi-parametric bootstrap approach described by Clauset et al. (2009).

A comparison of OLS estimates for three different low light DN thresholds illustrates some interesting changes in the rank-size distribution associated with different thresholds. Each column in Fig. 3 illustrates the effect of varying rank cutoff size on the value of the Zipf exponent (slope of the rank-size distribution) and linearity

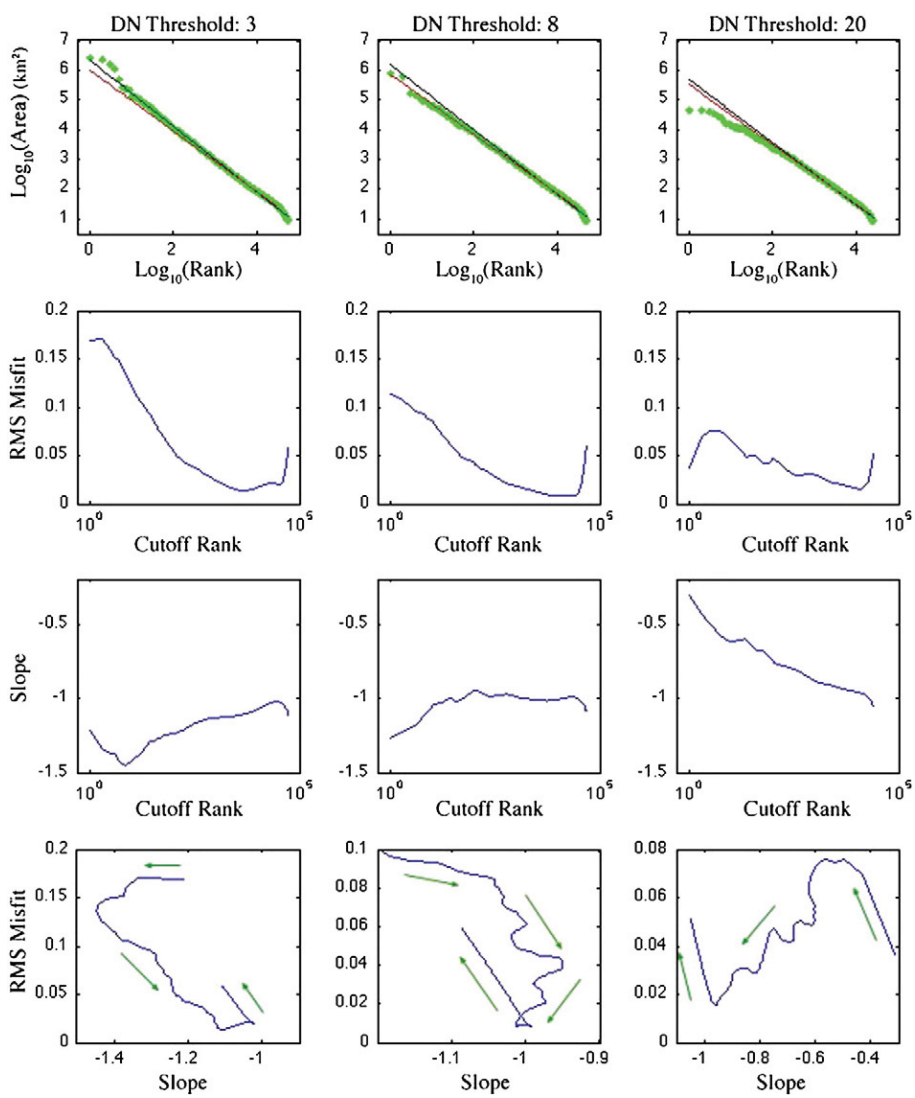

Fig. 3. Effect of increasing the number of agglomerations included in the upper tail of the rank-size distribution on the estimated slope and RMS misfit of the OLS estimate for different DN thresholds. Linear fits (top row) based on the upper tail cutoff rank with minimum RMS misfit (red) differ from those based on all agglomerations (black). For all DN thresholds RMS misfit diminishes until the large number of small agglomerations in the lower tail overwhelms the linear upper tail (2nd row). Hill plots show the dependence of the slope estimate on the number of agglomerations from the upper tail used in the estimate (3rd row). Trajectories of RMS misfit and slope for increasing number of agglomerations from the upper tail of the rank-size distribution all show misfit minima near the Zipf exponent (−1) before diverging as the lower tail is included in the estimate.

(Root Mean Square (RMS) misfit of the line to the data) for three different DN thresholds. In each case, both the slope and misfit are sensitive to the size cutoff used to define the upper tail of the distribution. For each DN threshold the RMS misfit diminishes with increasing cutoff rank (2nd row) through a series of local minima before abruptly increasing. This increase in misfit occurs at the point where the lower tail begins to exert greater influence on the exponent than the upper tail and the curvature evident in the lower tail causes abrupt increases in misfit. Similarly, the Hill plots showing the dependence of the exponent on the cutoff rank (3rd row) reveal a steady progression of the exponent toward −1 before diverging to steeper, more negative slopes as the lower tail assumes dominance of the fit near the same cutoff rank where the misfit blows up. Plotting the simultaneous trajectory of misfit and exponent for increasing cutoff rank (bottom row) illustrates the simultaneous convergence of both slope and linearity of the upper tail to the optimal cutoff where the lower tail begins to corrupt the fit. Note that the optimal slope is approached from below for the lower DN threshold and from above for the higher while the intermediate threshold of DN = 8 converges to a slope near −1 for cutoff ranks well under 100 and remains relatively stable until diverging for cutoff ranks greater than 10,000. The top row compares the rank-size distributions for different thresholds to both the optimal (minimum misfit preceding lower tail divergence) OLS linear fit (red line) and to the OLS fit to the entire sample population (black). Note the transition in the nature of the misfit of the uppermost tail—from exceeding the linear prediction (DN = 3) to matching it (DN = 8) to under estimating it (DN = 20).

5. Results

While the OLS approach is illustrative, it suffers from several shortcomings and biases (Clauset et al., 2009; Newman, 2005; Sornette, 2003). We therefore also use the MLE and semi-parametric bootstrap approach proposed by Clauset et al. (2009) to estimate the power law exponent and associated uncertainty, optimal rank cutoff for the upper tail and the goodness of fit for the suite of DN thresholds given above. This method is analogous to the OLS misfit optimization described above except that the power law exponent is estimated from the size distribution directly using the Maximum Likelihood estimator for each successive rank cutoff. The optimal slope estimate is that associated with the cutoff that minimizes the Kolmogorov–Smirnov (KS) statistic for the maximum difference between observed and Monte Carlo simulated power law distributions (Clauset et al., 2009). Goodness of fit is also determined using the KS statistic in a semi-parametric bootstrap algorithm that provides a statistical measure of plausibility for the power law hypothesis. For this goodness of fit test a p-value greater than 0.1 is considered indicative of a plausible fit (Clauset et al., 2009). For consistency and simplicity we transform the power law exponent (e) to the equivalent rank-size slope (s) as $s = 1/(e-1)$ (Li, 2002). Fig. 4 shows very similar dependence of the power law exponent and rank-size slope for the MLE and OLS estimates (respectively). In both cases DN thresholds greater than ~12 yield relatively consistent slopes > −1 but slopes increase abruptly as the threshold is reduced to DN = 3. This corresponds to a transition from distributions dominated by medium–large segments to increasingly connected distributions dominated by the very largest segments. The uncertainties (error bars) on the slope estimates and the goodness-of-fit statistic (p-values in italics) do not provide strong support for a power law distribution for DN thresholds >20 but 10 of 12 estimates for DN thresholds <20 are well-bounded with plausible goodness of fit. Both OLS and MLE estimates of the exponent show a rather abrupt transition from more uniform distributions at higher DN thresholds to steeper slopes and more uneven, large-segment-dominated distributions at lower DN thresholds.

The transition in exponent is also observed at continental scales for subsets of the global distribution. To investigate the robustness of the

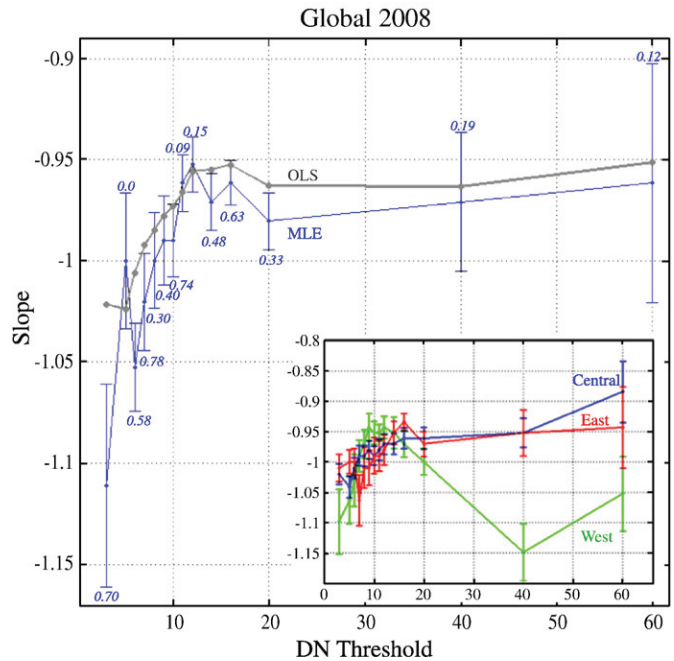

Fig. 4. Effect of low light thresholding on the slope of the rank-size distribution (or power law exponent). Reducing thresholds results in increasing coalescence of agglomerations as rank-size slope increases rapidly below DN = 12. Slope estimates from Ordinary Least Squares (OLS) in Log–Log space and Maximum Likelihood Estimation (MLE) of the power law exponent show the same progression and comparable slopes. Uncertainty bounds (bars) indicate transition across the Zipf exponent (−1) while P values greater than 0.1 (in italics) indicate plausible goodness of fit. Separate analyses of longitudinal subregions (inset) show similar progression with decreasing DN threshold.

transition in distribution at sub-global scales we divide the study area longitudinally along natural boundaries to avoid intersecting any spatial network of settlements. North, Central and South America are geographically isolated from Eurasia and Africa. Europe, western Asia, Arabia and Africa are longitudinally divisible from eastern Asia along a sinusoidal projection meridian intersecting the equator at 60°E. The purpose of the spatial subsetting is merely to verify the stability of the exponent and the transition observed in the global distribution—not to illustrate the myriad cultural, historical and socioeconomic differences between these regions. A more detailed analysis of country and regional scale distributions is the focus of a separate study. However, in spite of the many differences in urban structure and evolution, it is remarkable that the range and variation of the exponents are so similar at continental and global scales. The inset plots of slope versus threshold in Fig. 4 show analogous (but not identical) exponent transitions for three longitudinal subregions corresponding to the Americas (west), Europe, Africa and the Middle East (central) and Asia and Australia (east). All three subregions show abrupt transitions with decreasing DN threshold from shallower slopes (>−1) with more uniform size distributions to steeper slopes with more large-segment-dominated distributions. As in the case of the global analysis, the estimates for DN thresholds >20 have larger uncertainties and much lower p-values than those for DN<20. We note that the p-values merely indicate that the power law is a statistically plausible description of the data—not that it is necessarily the only, or even best, distribution that describes the data.

The transitions of the exponents through the Zipf case (−1) with decreasing DN threshold are manifest differently in the fits of the power law to the rank-size distribution for each subregion and for the global distribution. The examples given in Fig. 5 show cumulative probability distributions and the corresponding best fit power laws (from MLE) for DN thresholds of 3 and 12 as well as the threshold with the most Zipf-like (nearest −1) distribution (DN = 6, 7 or 8) for each of the three subregions and for the global dataset. In each longitudinal

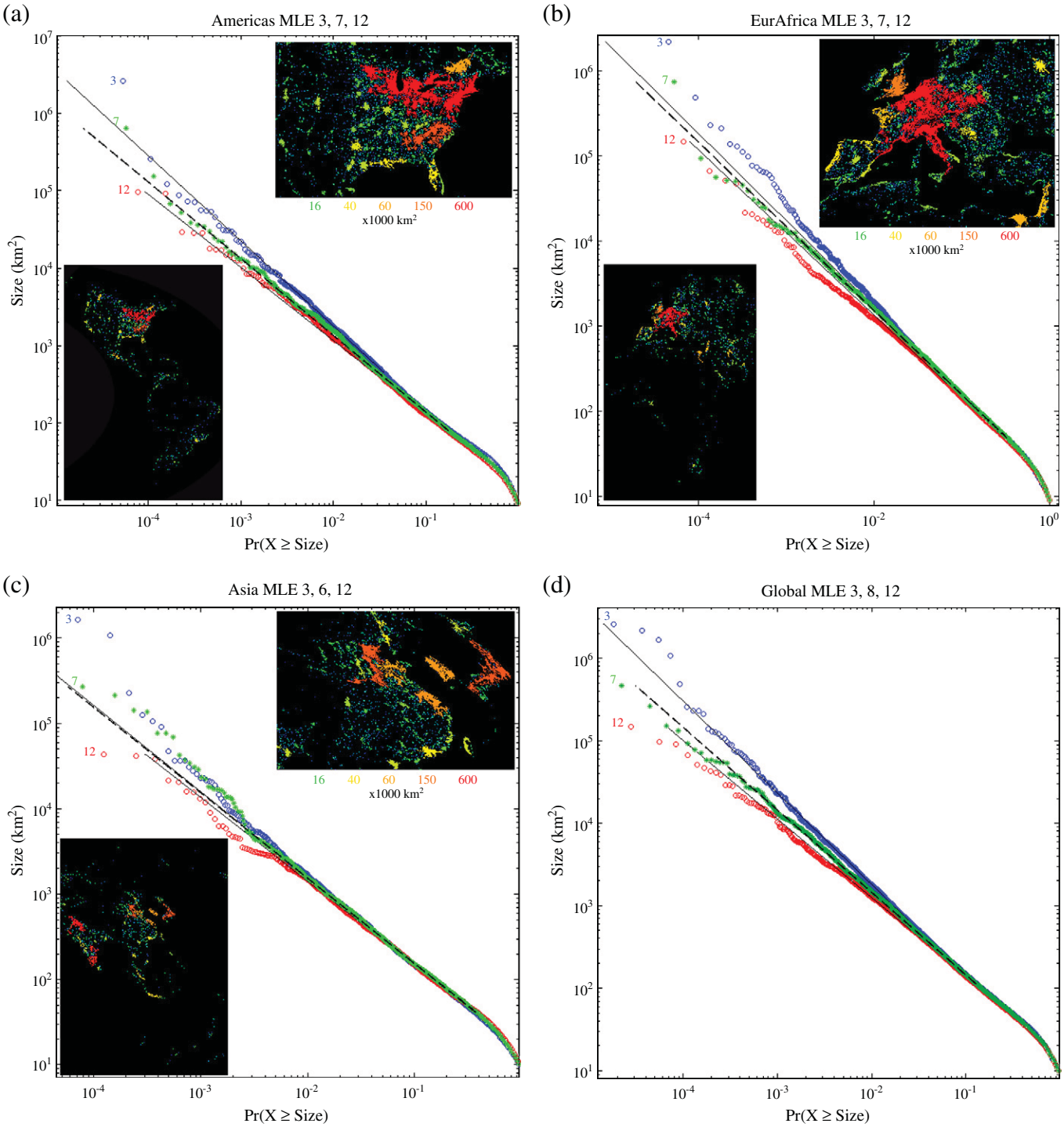

Fig. 5. a: Cumulative distribution functions and maximum likelihood power law fits for 3 low light thresholds spanning the Zipf exponent for the western longitudinal subset containing the Americas. Blue, green and red points correspond to DN thresholds of 3, 7 and 12 respectively. Inset maps show the segment size distribution of the DN = 8 threshold for the entire region (lower) and east-central North America (upper). The largest agglomeration is considerably larger than predicted by the power law for both DN thresholds 8 and 3 but the rest of the distribution is well fit. b: Cumulative distribution functions and maximum likelihood power law fits for 3 low light thresholds spanning the Zipf exponent for the central longitudinal subset containing Europe, Africa, Arabia and western Asia. Blue, green and red points correspond to DN thresholds of 3, 7 and 12 respectively. Inset maps show the segment size distribution of the DN = 8 threshold for the entire region (lower) and western Europe and N. Africa (upper). The largest agglomeration is considerably larger than predicted by the power law for DN thresholds 8 but the rest of the distribution is well fit. For the DN 3 and 12 thresholds the entire upper tail diverges from the linear prediction. c: Cumulative distribution functions and maximum likelihood power law fits for 3 low light thresholds spanning the Zipf exponent for the eastern longitudinal subset containing Asia and Oceania. Blue, green and red points correspond to DN thresholds of 3, 7 and 12 respectively. Inset maps show the segment size distribution of the DN = 6 threshold for the entire region (lower) and east Asia (upper). The largest agglomeration (northern India/Pakistan) is well predicted by the power law for DN threshold 6 but the rest of the upper tail is larger than predicted. d: Cumulative distribution functions and maximum likelihood power law fits for 3 low light thresholds spanning the Zipf exponent for the global light distribution. The DN = 8 threshold (green & dash) corresponds to a MLE estimated exponent of −1.00 and has a smaller misfit than any of the three longitudinal subregions.

subregion, the majority of the contiguous lighted agglomerations are associated with a single geographic region (or several regions in the case of Asia). The distribution for the Americas is dominated by the settlement network of eastern North America while the settlements in western North America and Central and South America contribute relatively little to the overall distribution. The same is true for Europe in comparison to the Middle East and Africa. Asia differs in the presence of at least five distinct regions containing settlement networks that combine to dominate the distribution. However, almost all the lighted area in Asia is concentrated in southern and eastern Asia.

The nature of the transition of each longitudinal subregion through the Zipf exponent with decreasing DN threshold differs in both the sensitivity of the slope (exponent) and the fit of the uppermost tail to the best fit power law. The transitions, along with the fits to the distributions are illustrated in Fig. 5. For each plot, we show distributions and best fit power laws for low (DN = 3), high (DN = 12) and transitional (DN = 7) thresholds. For each region, an inset map also shows the spatial segmentation associated with the threshold immediately preceeding the transition to extensive regional connectivity. A common transitional threshold is used for comparison among plots while regionally specific thresholds are used on the maps to illustrate the spatial form of the transition. For the Americas (Fig. 5a), the exponent of the best fit power law changes considerably with DN threshold although reasonable agreement between estimate and observation is obtained for all but the single largest agglomeration for each DN threshold. The inset maps show spatially contiguous lighted areas, color coded logarithmically by segment size, for the Zipf case with exponent closest to −1. North America is dominated by the contiguous agglomeration containing the Northeast Corridor and Great Lakes regions of the U.S.A and Canada. This spatial network is approximately five times the size predicted by the power law.

The distributions for Europe/Africa/Middle East (Fig. 5b) are very different from the Americas showing very little change in the best fit exponent but pronounced disparities in the fit of the upper tail to the power law. The DN threshold of 12 results in significant overestimate of the probability with even greater underestimation for the DN threshold of 3 while the Zipf case is well fit except for the single largest agglomeraton spanning western Europe from northern Germany to southern Italy. This spatial network is approximately three times the size predicted by the power law.

The distributions for Asia and Oceania (Fig. 5c) show a similar insensitivity of exponent to DN threshold with pronounced over and underestimation in the upper tail for lower and higher DN thresholds respectively. However the distributions for Asia differ from those of the central region in that the Zipf case is also not well fit in the uppermost tail. Approximately 30 agglomerations larger than ~10^4 km^2 are noticeably larger than predicted by the power law—although the largest agglomeration (northern India and Pakistan) fits the prediction very closely. Asia also differs from the other two longitudinal subsets in that its Zipf case contains several very large spatial agglomerations whereas the Americas and EurAfrica each contain only one. While the deviations of the largest agglomerations from the best fit power law are interesting, they do not detract from the excellent fits of the distributions to the power law. For any finite sample size the greatest deviations of observation from prediction are associated with the most extreme events (Sornette, 2003).

Interestingly, the combined global distribution (Fig. 5d) shows both greater sensitivity of the estimated exponent to DN threshold and noticeably better agreement between power law and observation in the upper tail. While there are a few prominent overestimations for DN = 3, the Zipf case (DN = 7) gives excellent agreement between model and observation. Note that in each longitudinal subregion the optimal rank cutoff corresponds to lighted segment areas considerably smaller than 100 km^2 while for the global distribution the optimal rank cutoff is a bit larger than 100 km^2. In every case, the power law provides a statistically plausible fit to the observed data for sample sizes greater than 10,000 segments spanning more than four orders of magnitude in each dimension suggesting that Zipf's Law provides at least as plausible a description of developed land area as it does for population count in prior studies. However, there are some important differences between these results and those of previous studies and these differences have implications.

6. Implications and conclusions

Zipf's Law holds for a wide range of developed land areas at both continental and global scales. The size distributions of agglomerations for the longitudinal subregions and the global aggregation are all well fit by power laws over more than four orders of magnitude in rank and size and all show similar transition of power law exponent with low light threshold. For the global distribution Maximum Likelihood estimates of the exponent range from −0.96 to −1.11 with plausible goodness of fit and uncertainty estimates clearly distinguishing a transition across the Zipf exponent of −1 with increasing low light threshold. Our results differ from those of Decker et al. (2007) because we are using a fundamentally different night light dataset. Decker et al. (2007) used an early 1994–95 version of the light data which did not benefit from numerous advances in processing developed by NGDC since 2000. The lower slopes found by Decker et al. (2007) are consistent with the higher detection limit of the older dataset which would reduce the connectivity at low light levels. For comparison, the analogous MLE estimate (using exactly the same method) of the power law exponent obtained by Clauset et al. (2009) for populations of U.S. cities in 2000 gives a rank-size slope of −0.73. We obtain a nearly identical value (−0.73) using the same MLE approach for a compilation of 19,032 global census counts used as the input to the Gridded Population of the World v.1 global population map (Tobler et al., 1997) . In both cases we attribute the lower slope of the population data to both the fragmented nature of the administrative units and to the relatively small fraction of the upper tail that yields the minimum misfit while excluding the lognormal lower tail that would tend to pull the slope higher. The estimates of population used in GPW version 1 are known to be far coarser than the true distribution (Balk and Yetman, 2004). However, both these population datasets designate cities on the basis of administrative boundaries thereby limiting potential size and contiguity with surrounding settlements. The implication is that Zipf's Law better explains spatial networks of settlements of varying size and density than it does discretized "cities" alone. Whatever underlying processes are responsible for the power law distribution, the processes clearly apply to spatial networks of varying types of anthropogenic land surface modification—not just "urban" areas.

Zipf's Law for developed land area extends beyond the scale of individual cities to much larger spatial networks of more intensely developed cities connected by less intensely developed suburban, peri-urban and rural areas. For the longitudinal subregions and the global aggregation, the closest agreement with the Zipf case (exponent of −1) spans more than four orders of magnitude in settlement size from small individual cities < 100 km^2 to large spatial networks > 1,000,000 km^2 of lighted land area encompassing a variety of different forms of anthropogenic modification. These spatial networks of development become vastly larger as the low light threshold diminishes to levels associated with peripheral and isolated settlements as well as less intensely developed interstitial regions. Yet these very large spatial networks still maintain a power law distribution with slopes near −1. While these very low levels of light are also associated with the peripheral overglow of larger settlements, the overglow generally encompasses areas with some anthropogenic modification. The increasing slope of the rank-size distribution indicates that the emergence of fewer, larger, interconnected agglomerations accounts for more total land area than smaller, more isolated and less extensively networked developments. This is in strong contrast to higher

thresholds where medium size networks and smaller isolated settlements account for most of the intensively developed land area. The implication is that Berry's concept of systems of cities (Berry, 1964) is manifest spatially through networks of development of varying intensity as implied by the notion of hierarchical systems as proposed by Pumain (Pumain, 2004, 2006) The size distributions of spatial agglomerations at all levels of development show a progression of connectivity that is dependent on the intensity of development. Across this range, the distribution is well fit by power laws with exponents very near −1. Recent and renewed attention to defining, measuring and understanding the socioeconomic characteristics of agglomerations (WorldBank, 2009; Glaser, 2010) is an important direction for understanding our future urban world.

Zipf's Law for developed land area is driven by the connectivity of localized regions of concentrated development. At continental to global scales the distributions of developed land areas are dominated by a few corridors of intense, space-filling development—in contrast to vast undeveloped areas containing few smaller isolated settlements or no significant development at all (e.g. ice sheets and deserts). These corridors of development, sometimes referred to as mega-regions, account for most of the formal economic activity on Earth (Florida et al., 2008). Most enumerated land area on Earth is inhabited at low population density (~70% area<10 people/km^2) (Small and Cohen, 2004)and large rural areas of intermediate population densities (100 to 1000 people/km^2) contain only small, isolated lights (Small, 2004). The interface or gradient between fully developed (e.g. "urban") and negligibly developed (e.g. "wilderness") is considerably less than it would be if this network were more extensively fragmented so that the distribution were dominated by smaller, less connected, more isolated settlements having even greater interface exposure. However, the interface exposure of the existing spatial network is far larger than it would be if the developed land area were more agglomerated rather than spatially networked. The limiting case for agglomeration would be a single giant circular settlement with minimum perimeter/area ratio. The implication is that anthropogenic development is a spatially networked phenomenon occurring across a wide range of spatial scales—but that the configuration of the network in any given location is influenced by multiple processes subject to geophysical, environmental, biological, evolutionary, cultural, economic and political constraints. The predictability of the size distribution does not necessarily imply the predictability of spatial configuration of the network at all (or even any) points. However, scholars of the spatial economy (Fujita et al., 2001) may be well positioned to leverage this knowledge.

Anthropogenic land cover development is consistent with the notion of a spatial phase transition from more isolated to more interconnected development patterns. The abrupt transition of the power law exponent with decreasing DN threshold is analogous to the transition observed in scaling exponents of percolation models (e.g. Stanley et al., 1999; Zallen, 1998; Newman, 2005). As in the case of percolation, the pronounced increase in the slope of the rank-size distribution corresponds to the increased spatial connectivity of the network of agglomerations as smaller patches become connected to form larger interconnected networks. This is the process responsible for the enormous size of the network bound by the lower light thresholds (DN<~8). If the process(es) of land cover development occur by some combination of isolated nucleation, edge expansion and intensification of previously developed land then some component of the growth and intensification process would follow a progression analogous to the spatial growth that results from lowering the brightness threshold. The concomitant increase in spatial extent would result in the transition in size distribution indicated by the abrupt decrease in the power law exponent. This is analogous to the abrupt increase in connectivity observed at critical points of spatial phase transitions. The concept of spatial phase transitions has been used to describe forest succession (Milne et al., 1996) and other ecological processes (Milne, 1998) and the concept of correlated percolation has been used to describe urban growth processes (Makse et al., 1995, 1998) with very encouraging results. Extending the concept of the spatial phase transition to include other forms of anthropogenic land cover modification and extending the spatial dimension to continental scales is consistent with the well-known fractal nature of urban development (Batty and Longley, 1986, 1994), the fractal nature of percolation processes (see e.g. Mandelbrot, 1982; Stanley et al., 1999) and the scale invariance associated with many other growth processes (see e.g. Stanley and Ostrowsky, 1986) and critical phenomena (see e.g. Sornette, 2003). Combining the percolation process with the notion of a continuum of land cover development provides a means representing the component of urban growth, and more generally land cover change, that proceeds by intensification of previously developed land area. The foundations for this concept are not new (see e.g. Batty and Longley, 1994) but, to our knowledge, have not been shown to operate at continental to global scales as implied by the distribution of lighted areas.

Anthropogenic light may provide a viable means for mapping the spatial extent and intensity of development worldwide. The DMSP-OLS was not designed for the purpose of mapping human settlements. Because the DMSP-OLS achieves a million fold amplification of the visible light level it enables the detection of sparse lighting located within large ground footprints of the individual pixels. One of the consequences of this extremely low detection limit and coarse spatial resolution is the detection of extensive areas of dim lighting in what are largely rural environments. The sources of this diffuse light are far smaller than the pixel footprint but their aggregate emission is detected nonetheless. This limits the size of the smallest detectable discrete objects but reveals their presence within the Instantaneous Field Of View of the pixel. This phenomena may account for the breakdown in the power law relationship in the lower tail of the distribution—along with differences in electrification (discussed below). Preliminary results of analyses of higher resolution population data and models suggest that the power law can be extended to finer spatial scales (Small et al., 2010). This could be verified using higher spatial resolution nighttime lights imagery. The potential for observing nighttime lights at moderate spatial resolution (~50 m) from space has been demonstrated with astronaut photography acquired from the International Space Station (Pettit, 2010). Elvidge et al. (2007a,b) have defined a Nightsat mission concept that would be capable of acquiring moderate resolution (50 m) color imagery of nighttime lights worldwide. Such data could be used to precisely map the location and morphology of sparse development worldwide.

It is important to note that the depiction of anthropogenic development in terms of light emission is far from perfect. The problem of overglow is well known. In addition to overglow, the night light data also contain some bright lights associated with gas flaring from oil production facilities (Elvidge et al., 2009). Another important consideration is the omission of settlements undetected by light emission. Much of subsaharan Africa is densely populated but not detected in the night lights. In spite of all these caveats, the rank-size distributions of lighted area across a wide range of brightness thresholds and at different spatial scales are consistently well fit by power laws with exponents very close to −1. Regardless of whether night lights depict population, economic activity, land cover modification or merely stable emitted light, the spatial distributions conforms to Zipf's Law more closely than most published studies using population data (Nitsch, 2005) and does so at global to continental scales. While the fit is certainly helped by the larger sample size (35,000 to 55,000 agglomerations for DN<12) of the light data, the large sample size would also provide stronger basis for rejection of Zipf's Law if it were spurious as suggested by some authors (e.g. Gan et al., 2006; Nitsch, 2005). Analogous analyses of global population density data (Small et al., 2010) yield results consistent with those reported here—despite the fact that population

density networks are different from those depicted by the lights. These preliminary analyses of population density and urban land cover with night lights reveal both consistencies and differences between spatially contiguous areas defined on the basis of night light, land cover and population density. A detailed comparison between these related entities is discussed in a separate study. We emphasize again that night lights provide a spatial analogue to population distribution that is both complementary and very different.

One of the most important caveats to consider when comparing night lights to population distribution is the importance of electrification to the prevalence of outdoor lighting. A recent study by (Dorelien et al., 2010) finds that urban extents based on night lights identify the overwhelming majority of highly electrified localities as measured from household questionaires in Demographic and Health Surveys. Recent analyses by (Doll and Pachauri, in press) indicate that large, dispersed rural populations in many developing countries do not have access to electricity and are therefore not represented in the night light data. This underscores the necessity to emphasize the distinction between population numbers and the varying area and intensity of land surface modification represented by different brightness levels of night light. While the two quantities may be correlated in areas that are brightly lit, the correlation says nothing about the large numbers of people living in areas where outdoor lighting detectable from space is either unavailable, unaffordable or not a cultural priority.

In summary, this analysis provides evidence supporting Zipf's law not only for cities but for larger, more inclusive spatial networks of urban and non-urban development. The results suggest a number of potential benefits should future studies of urbanization and land cover change embrace the notion of an urban continuum—one that includes small and large settlements as well as other types of land cover modification like agriculture that connect settlements in the form of spatial networks. The results further highlight the importance of integrating physical and social models of urban processes. To our knowledge, Zipf's law has not been used to forecast specific urban growth scenarios, but these findings suggest that spatial models of growth, and those that specifically acknowledge agglomerations and networks, may have predictive value.

Acknowledgements

This work was funded, in part, by the United States National Institutes of Child Health and Development award R21 HD054846 to the City University of New York, the Population Council and Columbia University. Additional support (to CS) was provided by the Doherty Foundation and the NASA Socioeconomic Data and Applications Center (SEDAC). The authors are grateful to three anonymous reviewers and to Aaron Clauset for helpful comments and suggestions.

References

Auerbach, F. (1913). Das Gesetz der Bevolkerungskonzentration. *Petermanns Geographische Mitteilungen*, *59*, 74—76.
Balk, D. (2009). More than a name: Why is global urban population mapping a GRUMPy proposition? In P. G. a. M. Herold (Ed.), *Global mapping of human settlement: experiences, data sets, and prospects*. Taylor and Francis.
Balk, D., & Yetman, G. (2004). The global distribution of population: evaluating the gains in resolution refinement. *Palisades, NY: Center for International Earth Science Information Network (CIESIN), Columbia University*.
Batty, M., & Longley, P. A. (1986). The fractal simulation of urban structure. *Environment and Planning A*, *18*, 1143—1179.
Batty, M., & Longley, P. (1994). *Fractal cities: A geometry of form and function*. San Diego, CA: Academic Press.
Berry, B. J. L. (1964). Cities as systems within systems of cities. *Papers in Regional Science*, *13*, 147—164.
Clauset, A., Shalizi, C. R., & Newman, M. E. J. (2009). Power–law distributions in empirical data. *SIAM Review*, *51*, 661—703.
Croft, T. A. (1973). Night-time images of the earth from space. *Scientific American*, *239*, 68—79.
Decker, E. H., Kerkhoff, A. J., & Moses, M. E. (2007). Global patterns of city size distributions and their fundamental drivers. *PLoS ONE*, *2*.
Doll, C. N. H., Muller, J. -P., & Morley, J. G. (2006). Mapping regional economic activity from night-time light satellite imagery. *Ecological Economics*, *57*, 75—92.
Doll, C. N. H., & Pachauri, S. (2010). Estimating rural populations without access to electricity in developing countries through night-time light satellite imagery. *Energy Policy.*, *38*, 5661—5670 doi:10.1016/j.enpol.2010.05.014.
Dorelien, A., Balk, D., Montgomery, M., & Todd, M. (2010). Conceptualizing and measuring urban location: comparing a satellite view with the demographic & health surveys. *Population Association of American Annual Meeting. Dallas, TX: PAA*.
Elvidge, C. D., Baugh, K. E., Kihn, E. A., Kroehl, H. W., & Davis, E. R. (1997). Mapping city lights with nighttime data from the DMSP operational linescan system. *Photogrammetric Engineering and Remote Sensing*, *63*, 727—734.
Elvidge, C. D., Cinzano, P., Pettit, D. R., Arvesen, J., Sutton, P., Small, C., Nemani, R., Longcore, T., Rich, C., Safran, J., Weeks, J., & Ebener, S. (2007a). The Nightsat mission concept. *International Journal of Remote Sensing*, *28*, 2645—2670.
Elvidge, C. D., Imhoff, M. L., Baugh, K. E., Hobson, V. R., Nelson, I., Safran, J., Dietz, J. B., & Tuttle, B. T. (2001). Night-time lights of the world: 1994–1995. *ISPRS Journal of Photogrammetry and Remote Sensing*, *56*, 81—99.
Elvidge, C. D., Safran, J., Tuttle, B., Sutton, P., Cinzano, P., Pettit, D., Arveson, J., & Small, C. (2007b). Potential for global mapping of development via a NightSat mission. *Geojournal*, *69*, 45—53.
Elvidge, C. D., Tuttle, B. T., Sutton, P. C., Baugh, K. E., Howard, A. T., Milesi, C., Bhaduri, B. L., & Nemani, R. (2007c). Global distribution and density of constructed impervious surfaces. *Sensors*, *7*, 1962—1979.
Elvidge, C. D., Ziskin, D., Baugh, K. E., Tuttle, B. T., Ghosh, T., Pack, D. W., Erwin, E. H., & Zhizhin, M. (2009). A fifteen year record of global natural gas flaring derived from satellite data. *Energies*, *2*, 595—622.
Florida, R., Gulden, T., & Mellander, C. (2008). The rise of the mega-region. *Cambridge Journal of Regions, Economy and Society*, *1*, 459—476.
Fragkias, M., & Seto, K. C. (2009). Evolving rank-size distributions of intra-metropolitan urban clusters in South China. *Computers, Environment and Urban Systems*, *33*, 189—199.
Fujita, M., Krugman, P., & Venables, A. (2001). *The spatial economy: Cities, regions and international trade*. Cambridge MA: MIT Press.
Gabaix, X. (1999). Zipf's law for cities: An explanation. *Quarterly Journal of Economics*, *114*, 739—767.
Gabaix, X., Ioannides, Y. M., Henderson, J. V., & Jacques-FranÁois, T. (2004). Chapter 53 The evolution of city size distributions. *Handbook of Regional and Urban Economics* (pp. 2341—2378). : Elsevier.
Gan, L., Li, D., & Song, S. (2006). Is the Zipf law spurious in explaining city-size distributions? *Economics Letters*, *92*, 256—262.
Glaser, E. (Ed.). (2010). *Agglomeration economics*. Chicago Il.: University of Chicago Press and National Bureau of Economic Research.
Guérin-Pace, F. (1995). Rank-size distribution and the process of urban growth. *Urban Studies*, *32*, 551—562.
Henderson, J. V., Storeygard, A., & Weil, D. N. (2009). Measuring economic growth from outer space. *National Bureau of Economic Research Working Paper*. Cambridge MA: NBER.
Imhoff, M. L., Lawrence, W. T., Stutzer, D. C., & Elvidge, C. D. (1997). A technique for using composite DMSP/OLS "city lights" satellite data to map urban area. *Remote Sensing of Environment*, *61*, 361—370.
Li, W. (2002). Zipf's law everywhere. *Glottometrics*, *5*, 14—21.
Makse, H., Havelin, S., & Stanley, H. E. (1995). Modeling urban growth patterns. *Nature*, *377*, 608—612.
Makse, H. A., Andrade, J. S., Batty, M. l., Havlin, S., & Stanley, H. E. (1998). Modeling urban growth patterns with correlated percolation. *Physical Review E*, *58*.
Mandelbrot, B. B. (1982). *The fractal geometry of nature.* New York: W. H. Freeman and Co.
Milne, B. T. (1998). Motivation and benefits of complex systems approaches in ecology. *Ecosystems*, *1*, 449—456.
Milne, B. T., Johnson, A. R., Keitt, T. H., Hatfield, C. A., David, J., & Hraber, P. (1996). Detection of critical densities associated with pin˜ on-juniper woodland ecotones. *Ecology*, *77*, 805—821.
Newman, M. E. J. (2005). Power laws, Pareto distributions and Zipf's law. *Contemporary Physics*, *46*, 323—351.
Nitsch, V. (2005). Zipf zipped. *Journal of Urban Economics*, *57*, 86—100.
Overman, H. G., & Ioannides, Y. M. (2001). Cross-sectional evolution of the U.S. city size distribution. *Journal of Urban Economics*, *49*, 543—566.
Pettit, D. (2010). Cities at night: An orbital perspective. *NASA Ask Magazine*.
Pumain, D. (2004). Scaling laws and urban systems. In (p. 26). Santa Fe NM: Santa Fe Institute.
Pumain, D. (2006). Alternative explanations of heirarchical differentiation in urban systems. In D. Pumain (Ed.), *Hierarchy in natural and social sciences* (pp. 169—222). Dordrecht Germany: Kluwer.
Pumain, D., & Moriconi-Ebrard, F. (1997). City size distributions and metropolisation. *Geojournal*, *43*, 307—314.
Rosen, K. T., & Resnick, M. (1980). The size distribution of cities: An examination of the Pareto law and primacy. *Journal of Urban Economics*, *8*, 165—186.
Rozenfeld, H. n. D., Rybski, D., Andrade, J. S., Batty, M., Stanley, H. E., & Makse, H. n. A. (2008). Laws of population growth. *Proceedings of the National Academy of Sciences*, *105*, 18702—18707.
Small, C. (2004). Global population distribution and urban land use in geophysical parameter space. *Earth Interactions*, *8*, 1—18.
Small, C., & Cohen, J. E. (2004). Continental physiography, climate, and the global distribution of human population. *Current Anthropology*, *45*, 269—277.
Small, C., Pozzi, F., & Elvidge, C. D. (2005). Spatial analysis of global urban extent from DMSP-OLS night lights. *Remote Sensing of Environment*, *96*, 277—291.

Small, C., Montgomery, M., Balk, D., Elvidge, C., Bright, E., & Yetman, G. (2010). Global scaling and connectivity of human population and development. *Submitted to Proceedings of the National Academy of Sciences*.

Soo, K. T. (2005). Zipf's Law for cities: A cross-country investigation. *Regional Science and Urban Economics*, *35*, 239−263.

Sornette, D. (2003). *Critical phenomena in natural sciences*, 2nd Ed. Heidelberg: Springer-Verlag.

Stanley, H. E., Andrade, J. S., Jr., Havlin, S., Makse, H. n. A., & Suki, B. (1999). Percolation phenomena: A broad-brush introduction with some recent applications to porous media, liquid water, and city growth. *Physica A: Statistical and Theoretical Physics*, *266*, 5−16.

Stanley, H. E., & Ostrowsky, N. (Eds.). (1986). *On growth and form: Fractal and non-fractal patterns in physics*. Dordrecht: NATO.

Sutton, P., Roberts, D., Elvidge, C., & Baugh, K. (2001). Census from heaven: An estimate of the global human population using night-time satellite imagery. *International Journal of Remote Sensing*, *22*, 3061−3076.

Sutton, P., Roberts, C., Elvidge, C., & Meij, H. (1997). A comparison of nighttime satellite imagery and population density for the continental united states. *Photogrammetric Engineering and Remote Sensing*, *63*, 1303−1313.

Tobler, W., Deichmann, U., Gottsegen, J., & Maloy, K. (1997). World population in a grid of spherical quadrilaterals. *International Journal of Population Geography*, *3*, 203−225.

WorldBank (2009). World Development Report: Reshaping Economic Geography. In. Washington D.C.: World Bank.

Zallen, R. (1998). *Physics of amorphous solids.* New York: Wiley.

Zipf, G. K. (1949). *Human behavior and the principle of least-effort.* Addison Wesley.